Adaptive High-order Wavefront Control Algorithms for High-contrast Imaging on the Decadal Survey Testbed

K. Cahoy
Co-Investigators: L. Pogorelyuk, R. Soummer, L. Pueyo, J. Kasdin
Collaborators: B. Nemati
Graduate Students: S. Redmond, C. Page, A. Meredith

1. Contents

Approval page

Prepared by:

Kerri Cahoy **10/27/2023**
Dr. Kerri Cahoy
Principal Investigator
Professor
Department of Aeronautics and Astronautics
Massachusetts Institute of Technology

Approved by:

_____
Dr. Brendan Crill
Deputy Program Chief Technologist
Exoplanet Exploration Program
NASA/Jet Propulsion Laboratory
California Institute of Technology

_____
Dr. Nicholas Siegler
Program Chief Technologist
Exoplanet Exploration Program
NASA/Jet Propulsion Laboratory
California Institute of Technology

_____
Dr. Douglas Hudgins
Program Scientist
Exoplanet Exploration Program
Science Mission Directorate
NASA Headquarters

2. Objective

The objective of this work is to achieve the success criteria of Technology Readiness Level (TRL) 4 of dark hole maintenance (DHM) with respect to the Habitable Worlds Observatory (HWO) recommended by the "Pathways to Discovery in Astronomy and Astrophysics for the 2020s" decadal survey (Astro2020). DHM belongs to a family of "Adaptive wavefront control algorithms that are more efficient and improve tolerance to instabilities," which is one of the "high-priority technologies to mature" identified by Astro2020.

This work will be conducted on both the High-contrast Imager for Complex Aperture Telescopes (HiCAT) testbed at Space Telescope Science Institute (STScI) and the Decadal Survey Testbed (DST) at Jet Propulsion Laboratory (JPL). We have matured DHM to a TRL of 3 by demonstrating baseline functionality on HiCAT in air [Redmond et al. 2022] at contrast better than 10^{-7}. The objective of this work is to achieve the success criteria of TRL to 4 by demonstrating DHM in vacuum at contrast better than 10^{-9}. This will require:

1. Prediction of optimal DHM performance on the optical model of HiCAT and under various wavefront aberrations and light intensities.
2. Development of (near-)optimal DHM algorithms and their validation on HiCAT at ~10^{-8} contrast.
3. Deployment of selected DHM algorithms on DST at ~10^{-10} contrast and comparison to theoretical predictions.

3. Introduction and Background

Astro2020 recommends searching for life signatures on exoplanets using a large aperture space telescope equipped with a coronagraph. The coronagraph would need to be capable of detecting light from planets that are 10^{-10} times dimmer than their host stars [Stark et al. 2019]. NASA has made significant progress in demonstrating that this 10^{-10} contrast can be achieved with modern optical elements [Seo et al. 2019]. However, there remains much work to demonstrate that this delicate contrast can be maintained in the presence of high-order optical disturbances such as primary mirror deformations and deformable mirror actuator drift.

The Coronagraph on the Roman Space Telescope will operate in a "set and forget" scheme: it will obtain its peak contrast of about 10^{-8} when pointing at a bright reference star, then point to a dimmer target star while the contrast slowly deteriorates, then point back periodically at the reference star for recalibration several times a day [Kasdin et al. 2020]. While reasonable at 10^{-8} contrast, this approach is very unlikely to be feasible on larger telescopes at 10^{-10} contrast. First, assuming high-order wavefront disturbances similar to those on JWST, a 10^{-10} contrast would need to be recalibrated on time scales of seconds to minutes (see Fig. 1). On the Decadal Survey Testbed (DST) at the Jet Propulsion Laboratory (JPL), for example, the contrast deteriorates by an unacceptable 10^{-10} within the first hour of operation after calibration without an update [Meeker et al. 2021]. Second, even if there were a mechanism for quickly repointing the observatory between target and reference stars, it would introduce significant complexity to the mission and itself inject high-order optical disturbances that may not be able to be sensed by onboard metrology.
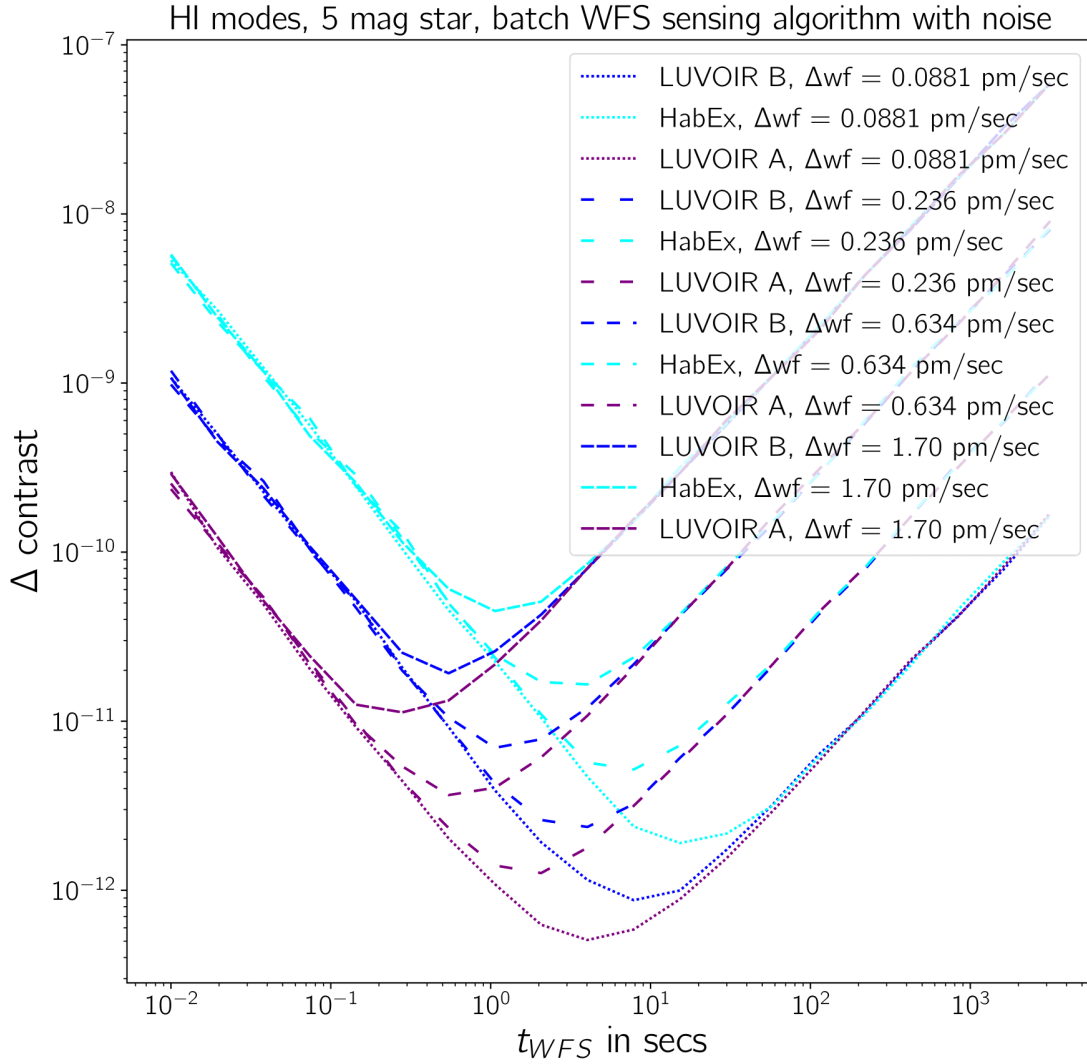
Figure 1. Analytical estimates of the impact of high-order wavefront drift of various magnitudes on the contrast of HabEx and LUVOIR. The performance is measured in terms of contrast delta between the initial contrast achieved by the coronagraph in the absence of time-varying wavefront errors (WFE) and the closed-loop contrast maintained by high-order wavefront estimation and control in the presence of WFE drift. The contrast delta depends on the WFE drift and the signal-to-noise-ratio (SNR) of the detector (in this figure and the proposed work, we assume that the SNR is dominated by shot noise which depends on exposure time). *From Pueyo et al. 2021*

There are many modes of optical disturbances that will be addressed via a multi-tiered wavefront control system in the future observatory. High-order disturbance modes include deformable mirror (DM) actuator drift [Prada et al. 2019] and relative shifts of far-apart mirror segments [Laginja et al. 2022]. These perturbations are not sensed by existing dedicated low-order wavefront sensors or inter-segment sensors [Coyle et al. 2022] (both are non-common path sensors). Instead, these numerous high-order wavefront perturbations are addressed with high-order wavefront sensing and control (HOWFSC).

HOWFSC uses images from the science camera to update the shapes of deformable mirrors to create a high-contrast region in the image known as the dark hole (DH).

The HOWFSC algorithms that will be deployed on Roman coronagraph are Pairwise Probing and Electric Field Conjugation (EFC) [Give'on et al. 2007]. They will estimate the electric field of the starlight in the DH and reduce its intensity. With some modifications, these algorithms can also continuously maintain the high contrast in the image while observing the target star [Pogorelyuk & Kasdin 2019]. This work will thoroughly examine these baseline algorithms in the presence of various wavefront drift rates and shot noise strengths (see Fig. 1 and Table 1).
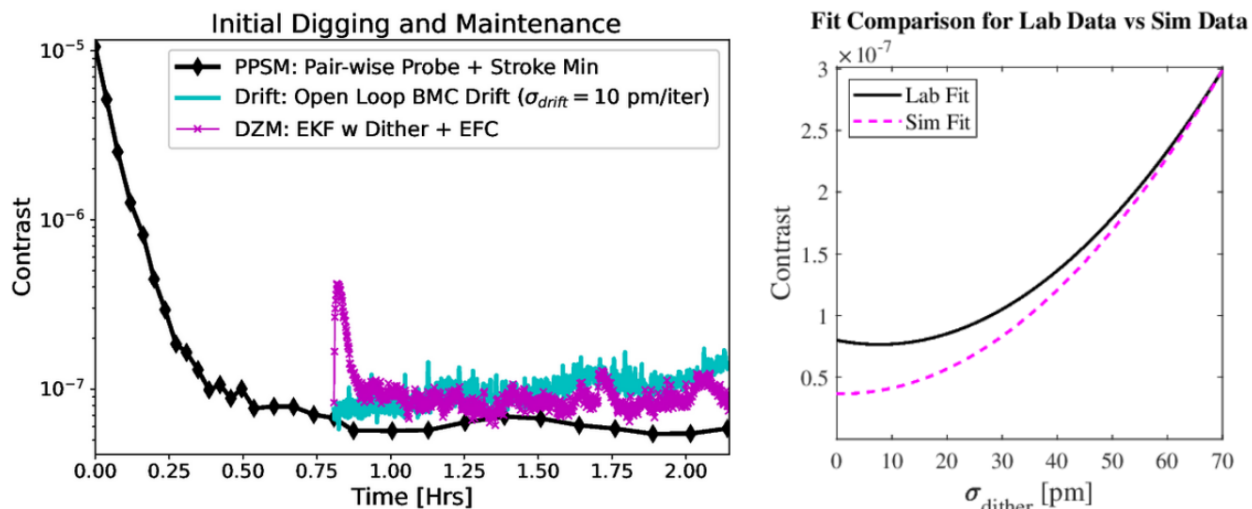
Figure 2. Our demonstration of dark hole maintenance on HiCAT in air (TRL 3) at 8 x 10⁻⁸ contrast. Left: The process of DH creation on HiCAT (black line), followed by Dark Zone Maintenance (DZM — same as DHM) utilizing an Extended Kalman filter (EKF; magenta line) with artificially introduced wavefront drift via the Boston Micromachines (BMC) DMs (teal line in open loop) and relatively low photon flux. The DHM experiences a transient period during which the estimator converges before the contrast becomes stable. Right: Comparison of closed-loop performance between lab and simulations for various values of a tunable controller parameter (magnitude of DM probes/dither necessary to introduce phase diversity). *From Redmond et al. 2022.*

We demonstrated this baseline Dark Hole Maintenance (DHM) scheme on HiCAT [Redmond et al. 2022] in 2021 as shown in Fig. 2. We conducted this preliminary experiment at a contrast of 8×10^{-8}, a segmented primary surrogate, a Lyot coronagraph, and low SNR (low photon-flux) conditions at 640 nm and 3% bandpass. We introduced wavefront disturbances via two types of deformable mirrors: continuous Boston Micromachines (representative of monolithic-mirror shape perturbations) and IrisAO (representative of segment-level mirror piston/tip/tilt perturbation). Our DHM algorithm [Pogorelyuk & Kasdin 2019] then compensated for those disturbances using science-camera images alone (magenta line on Fig. 2, left). The performance of DHM on the testbed matched its performance on the high-fidelity numerical model of HiCAT (Fig. 2, right) within a factor of 2.

Yet, the baseline DHM algorithms are suboptimal, as we have shown in a simulation of the Roman Coronagraph based on Observing Scenario 9 [Pogorelyutk et al. 2022]. The baseline estimation

technique (pairwise probing) uses information from just a single pixel to estimate the speckle electric field at that pixel. When the cross-correlation between pixels is ignored, larger DM probes are necessary to overcome shot noise and estimate the electric field with sufficient SNR for wavefront control. Large probes, in turn, result in higher contrast loss, over an order of magnitude larger than theoretical lower bounds that consider pixel cross-correlation. To raise confidence in the optimistic theoretical predictions of closed-loop (e.g., Fig. 1), we aim at deploying advanced algorithms on HiCAT and DST that include near-optimal wavefront sensing and control (and system identification approaches if the testbed performance falls significantly short of theoretical predictions due to testbed-model mismatch).

4. Milestones Description

Table 1. Milestone testbed, algorithms, and experiment parameters. Note that DM dither (or probe) magnitude is a controller tuning parameter that will be optimized across several trials for a given set of experiment parameters.

Milestone	Goal	Testbed/Environment	Algorithms	Parameter Range
1	Identify gap between theory and experiment	HiCAT in air; contrast better than 10^{-7} (TRL >3)	Baseline [Pogorelyuk & Kasdin 2019]	DM drift: 30 pm to 3000 pm per iteration shot noise: 0.3 to 30 SNR
2	Reduce gap between theory and experiment	HiCAT in air; contrast better than 10^{-7}	Advanced (a combination of algorithms described in Sec. 5.2)	at least one decade from each parameter range in milestone #1
3	Identify gap between theory and experiment	DST in vacuum; contrast better than 10^{-9}	Baseline	TBD (at least one decade in drift and shot noise)
4	Reduce gap between theory and experiment	DST (TLR 4)	Advanced	Same as in milestone #3

4.1 Milestone #1

Identify the gap between closed-loop dark hole maintenance performance on HiCAT (in air) and theoretical limit based on HiCAT model. *Determine theoretical closed-loop bound on the contrast (loss) delta in the presence of a) artificial wavefront instabilities from 30 to 3000 pm introduced on the Boston DM between every two exposures and b) shot noise with average SNR from 0.3 to 30 introduced in HiCAT software after each exposure. Determine the contrast delta starting from $8x10^{-8}$ or better that is*

achievable in practice on HiCAT with baseline dark hole maintenance algorithm for the above range of wavefront drift and shot noise.

We will compute lower bounds on contrast delta via the method presented in Pogorelyuk et al. 2021 using the HiCAT model. This bound requires a linear model of how WFE affect the electric field in the dark hole but it is independent of the wavefront control algorithm and tuning parameters. The contrast delta is higher for larger wavefront drift or higher shot noise. We will then run the baseline DHM algorithm on HiCAT over the specified range of wavefront drift and shot noise, as well as algorithm-specific tuning parameters (DM dither magnitude and EFC regularization). The experimental delta is expected to be significantly larger than the theoretical bound based on numerical simulations of baseline DHM [Pogorelyuk et al. 2022]. By the end of Milestone #1, we will understand the discrepancies between the best contrast deltas obtained on the testbed and the theoretical bound.

4.2 Milestone #2

Reduce the gap between closed-loop dark hole maintenance performance on HiCAT and theoretical limit. *Demonstrate that advanced algorithms can achieve a closed-loop contrast delta within a factor of 5 of the theoretical bound on HiCAT (identified in Milestone #1). This within-factor-of-5 performance will be demonstrated over a) at least one decade (factor of 10 between the start and end of the range) of artificial wavefront instabilities within the larger range of 30 to 3000 pm introduced on the Boston DM between exposures and b) at least one decade of average shot noise SNR within 0.3 to 30 introduced in HiCAT software after each exposure.*

The factor-of-5 performance of closed-loop contrast is with respect to a theoretical bound in Pogorelyuk et al. 2021. However, this bound might not be tight or achievable in practice because it does not take into account image probes that are necessary to resolve phase ambiguities in the electric field. Figure 3 suggests that the actual bound (that includes probes) could be higher by a factor of 3 of the theoretical bound (that does not).

We will consider several advanced approaches, as described in Section 5.2, that would make more efficient use of the available measurements to achieve a lower contrast delta compared to baseline DHM (after tuning their respective parameters). Based on our experiments for milestone #1, we will have a better understanding of the sub-range of conditions under which it makes sense to test the advanced DHM algorithms:

- In milestone #2, we aim at reducing the contrast delta gap for at least one decade (for example, 50 to 500 pm) from the 30 to 3000 pm drift range prescribed on the DM in milestone #1.
- In milestone #2, we aim at reducing the contrast delta gap for at least one decade from the 0.3 to 30 SNR range of shot noise added in milestone #1.

4.3 Milestone #3

Baseline Dark Hole Maintenance on DST. *Run baseline DHM algorithms in vacuum on the DST (similar to milestone #2). Starting with a contrast of $4x10^{-10}$, if possible, or the highest consistently reproducible on the DST at the time of the experiment. Perform a parameter scan of at least one decade*

of wavefront drift values and one decade of shot noise SNR. Identify the gap between closed-loop dark hole maintenance performance and theoretical limit based on the DST model.

The experimental setup and algorithms used will depend on the hardware available on the DST and lessons learned while completing milestones #1 and #2. The DST coronagraph will not necessarily be the same type as on HiCAT (the type of the coronagraph does not affect our analysis of algorithms). Before the lab experiments, we will deploy baseline DHM algorithms on the optical model of the DST and compare them to theoretical predictions. We will then run baseline DHM algorithms for a wide range of wavefront drift values and shot noise SNR (over one decade each). This will help determine a range of parameters over which we will compare advanced DHM algorithms to theoretical prediction (similar to the transition from milestone #1 to #2).

4.4 Milestone #4

Dark Hole Maintenance at TRL 4 on DST. *Demonstrate that advanced algorithms can achieve a closed-loop contrast delta within a factor of 5 of the theoretical bound on DST (identified in Milestone #3).*

The lab setup will remain the same between milestones #3 and #4 . Before the lab experiments, we will deploy selected (based on milestone #2) advanced DHM algorithms on the optical model of the DST and compare them to theoretical predictions.

5 Experiment Description

5.1 Parameter scan of baseline DHM algorithm on HiCAT
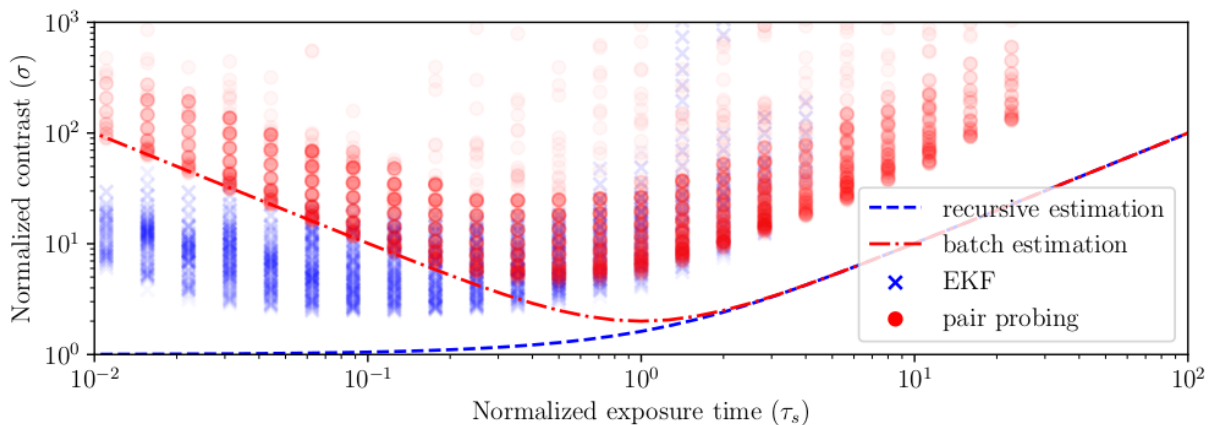
Figure 3. A parameter scan of a dark hole maintenance for a numerical example (one-pixel dark hole; pairwise probing based on Give'on et al. 2007 is marked by o, and EKF based on Pogorelyuk & Kasdin 2019 is marked by x) and comparison to theoretical predictions (lines). The closed-loop contrast depends on the exposure time normalized by E-field drift rate, as well as on the tuning parameters of the estimator

and controller including probe magnitude. The optimal performance gets within a factor of 3 of the theoretical bound. This work will begin with a similar parameter scan on the HiCAT testbed with all pixels included instead of just one (on HiCAT, we will tune the algorithms much more carefully than in this example to reduce the number of runs). *From [Pogorelyuk et al. 2021]*

Our goal is to quantify the gap between model-based theoretical predictions and testbed performance when it comes to closed-loop contrast loss due to wavefront drift (contrast delta). HiCAT consistently achieves a contrast of at least 8×10^{-8} in monochromatic light in air [Soummer et al. 2022]. It can be operated remotely, which makes it ideal for running large parameter scans. While we will aim at obtaining the best contrast before running DHM, we also realize that testbed performance is not always reproducible between experiments. We will therefore accept 8×10^{-8} contrast averaged over a half-annulus black hole between 4.7 and 12 lambda/D as a minimum requirement. We will perform our experiments in broadband light if this contrast can be achieved with 10% spectral bandwidth. Note that on both HiCAT and DST, the contrast will hit its limit *before* running DHM and, therefore, will not undermine our conclusions about the performance of DHM itself.

The DHM algorithm will run after a dark hole is created using standard procedures (pairwise probing and EFC). DHM is insensitive to coronagraph type and bandwidth. We will choose a configuration that is well suited for achieving milestone #1, then run the baseline DHM algorithm [Pogolreyuk & Kasdin 2019, Redmond et al. 2022] while applying random walk on each of the Boston DM actuators with increments of 30 to 3000 pm RMS between iterations. We will take high SNR images of the dark hole (at a high SNR laser setting) and add shot noise in software. We will scale the images such that the SNR of the added shot noise will range from 0.3 to 30, averaging across all dark-hole pixels.

In order to close the wavefront control loop, DHM applies random DM probes (or dithers the DM) similar to probes that are applied on the DM during the dark hole creation process. DHM may stabilize the contrast at a certain level if the DM dither is large enough (below that, the contrast deteriorates indefinitely). For a given setup, the optimal dither magnitude depends on the drift rate and the measurement noise SNR. Very large dither increases the contrast delta, while a very small dither does not result in a stable dark hole. Overall, we will explore a 3-dimensional space: scan the two dimensions of drift and SNR values, and search for the optimal dither value in each case, similar to the parameter scan in Fig. 2. We will report the closed-loop contrast deltas for optimal dither values for the drift and SNR values. We will then use the analytical approach described in [Pogorelyuk et al. 2021] and a model of HiCAT to compute a theoretical bound on the contrast deltas for the parameters in Table 1 (note that theoretical bounds do not rely on DM dither).

5.2 Advanced DHM algorithms for close-to-theoretical contrast delta on HiCAT
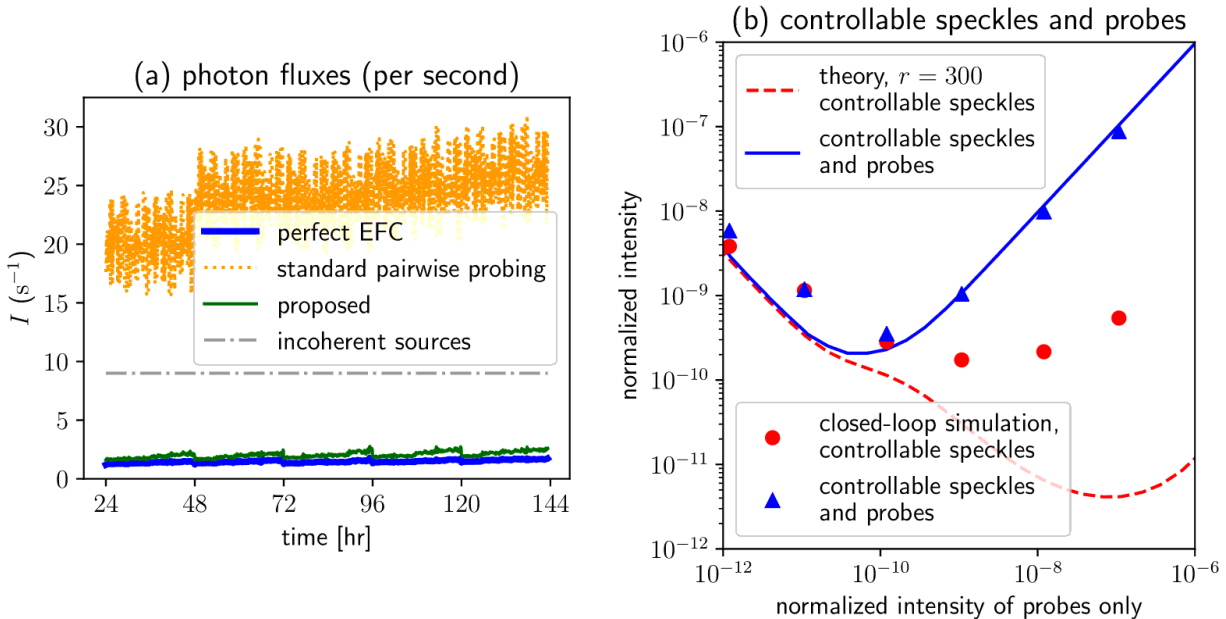
Figure 4. Simulations of dark hole maintenance on Roman Coronagraph based on Observing Scenario 9 (OS9) data. (a) Baseline algorithm, pairwise probing (single-pixel estimation), requires probing the DM to estimate the electric field of the starlight speckle in the dark hole. However, these probes need to be very large to maintain a fixed contrast − the normalized starlight photon flux in the dark hole. This results in a contrast that is much larger than if the electric field was known in simulation (perfect electric field conjugation − EFC), although this discrepancy could potentially be mitigated by using the more advanced estimation and control algorithm proposed in Pogorelyuk et al. 2022 (modal EFC). (b) Modal EFC (simulation results are marked by circles and triangles) achieves its optimal performance with smaller probes and therefore gets closer to theoretically predicted performance (lines). *From [Pogorelyuk et al. 2022].*

The baseline algorithms for estimating the electric field of the speckles are single-pixel (pairwise probing and extended Kalman filter running with data from one pixel at a time). Our numerical simulations (Fig. 4) suggest that the corresponding baseline closed-loop contrast delta is over 40 times higher than the theoretical bounds. Our previous experiments [Redmond et al. 2022] also show discrepancies of up to a factor of 2 between DHM performance in the optical model and on the testbed.

Our goal for milestone #2 is therefore, to minimize two gaps: a) the gap between theoretical predictions *based on* the optical model of HiCAT and DHM performance in simulations, and b) the discrepancies between DHM performance in simulations and on the testbed. In the end, we aim at a testbed performance within a factor of 5 (in terms of contrast delta) between theoretical predictions and testbed performance (both gaps combined). This goal will be achieved by one or more of the following means:

- *Modal wavefront control and estimation.* We will begin with the modal EFC algorithm proposed in Pogorelyuk et al. 2022 and which takes into account the cross-correlation *between* dark hole pixels when estimating the electric field and controlling it. This is done by posing a better-conditioned joint estimation and control problem in terms of a smaller number of modes. Better use of noisy measurements allows for DHM with lower DM probes and hence lower impact on closed-loop contrast compared to baseline (single-pixel) algorithms.
- *System identification.* The modal EFC approach requires a sufficiently good model of the testbed — in particular the electric field Jacobian that is computed via an optical simulation. If we do not achieve a contrast delta within a factor of 5 from theoretical results, it could be due to a large mismatch between numerical simulation and testbed performance (e.g., a factor of 4 in simulations and a factor of 8 on the testbed, similar to the factor 2 difference we previously reported in Redmond et al. 2022). In that case, we will deploy system-identification algorithms such as the one proposed in Sun et al. 2018 (tested experimentally at 2×10^{-7} contrast) to get a better Jacobian based on empirical measurements. These system ID algorithms will take measurements without any drift or noise introduced. The more accurate Jacobian will be used with modal EFC to try to reach the goal of factor 5 contrast delta.
- *Jacobian-free methods.* Finally, If modal EFC does not reach the desired performance and if time allows it, we will consider algorithms that do not rely on the model-based Jacobian. These include the implicit EFC [Haffert et al. 2023], as well as any other algorithms available at the time.

After testing advanced algorithms with DM drifts described in Table 1, we will also test them *in a simulation* of drift on the segmented IRIS-AO. The magnitude of the segment tip, tilt, and piston drifts will be chosen to match the open-loop contrast deterioration rate of one of the experiments with DM drift. While possible in simulation, such drift magnitude would currently be below the stroke resolution of the IRIS-AO on HiCAT.

Keeping the IRIS-AO drift magnitude constant, we will perform a parameter scan of advanced DHM algorithms of at least one decade of shot noise SNR. This will require computing the IRIS-AO Jacobian (the "modes" that appear in the formulation of modal EFC) in addition to the DM Jacobian. By design, the IRIS-AO modes are controllable by the DM therefore, we do not expect a degradation in the performance compared to the DM drift.

5.3 DHM algorithms on the DST

Based on our experience on HiCAT, we will choose the DHM approach, and potentially a system identification approach, that are most likely to yield closed-loop performance close to theoretical limits. By the time we have access to the DST, we will have implemented the selected algorithms in an optical model of the DST (FALCO [Riggs et al. 2018]). Since the algorithms are coronagraph-architecture independent, we will be able to choose the coronagraph close to the beginning of the experiments (the algorithms do require the Jacobian corresponding to the coronagraph and dark hole geometry, whatever it may be). Our algorithms [Pogorelyuk & Kasdin 2019, Pogorelyuk et al. 2022] can easily switch between 3 modes:
- monochromatic light — laser source with single-channel detectors (single wavelength electric-field Jacobian)

- Roman-like setup — broadband light with single-channel detectors (multiple wavelengths electric-field Jacobian)
- fully broadband setup — broadband light with the measurement at multiple spectral channels (multiple wavelength electric-field Jacobian). In the absence of an Integral Field Spectrograph (IFS), this can be achieved by changing spectral filters sequentially between exposures, although this might not be feasible when running tens of thousands of control iterations.

The DST can switch between monochromatic and broadband imaging during the experiment. However, the contrasts vary by an order of magnitude between the two modes [Seo et al. 2019, Ruane et al. 2022], and may differ from experiment to experiment in the same mode. Before running DHM, we will obtain the highest possible contrast on DST. We will aim at testing DHM with a starting contrast of at least 8 x 10^{-10} averaged over at least a circle-segment dark hole from 4 to 10 lambda/D and operating at a 10% fully-broadband setup, if feasible. If a fully-broadband setup is not feasible, we will revert to a Roman-like setup or a monochromatic source and the highest achievable contrast otherwise.

The DST currently employs Charge-Coupled Device detectors (CDDs) rather than the Electron Multiplying CCD (EMCCD) detectors used, for example, on Roman. EMCCD and CCD have different noise profiles. Depending on the detector available on the DST at the time of the experiment, we will scale the exposure times such that the magnitude of the noise on the DST is representative of the shot noise on the HWO. If necessary, we will use DST's capability of introducing neutral density filters to reduce the photon flux, or add artificial noise in software. Similar to HiCAT, we will use DM actuators to both introduce and correct the WFE. The contribution of the DM to the WFE will not be "known" to the estimator and the controller, whose corrections (and DM probes) will be applied "on top" of the drift.

Additionally, and to the extent allowed by export control, we will provide the community with a data package similar to Observing Scenario 9 [Krist, 2020] on the IPAC website (see Sec. 6.3). It will include a data sequence of images taken on DST; control, drift, and probe voltages applied on the DM, the DM Jacobian used, and the estimation and control parameters. Using this data, we will be able to make initial predictions for the performance of HWO. The data produced in our DH maintenance experiments will be scaled such that it is representative of various potential wavefront instabilities and detector noise on the HWO.

6 Data Measurement and Analysis

6.1 Definitions

Initial contrast: The contrast is defined as the averaged light intensity of the dark hole divided by the maximum intensity of the entire unobscured image (with the coronagraph mask removed). Before each experiment, the contrast will be minimized using existing dark hole creation techniques. The contrast at the beginning of the experiment is the "initial contrast."

Wavefront control iteration: An iteration is a logical time unit during which wavefront drift is applied on the DM, a measurement is taken with the science camera, shot noise is applied in software, an estimator algorithm is advanced, a control output is computed, and DM corrections are prepared for the next iteration. The physical duration of each iteration is not considered in the context of this work.

Deformable mirror software values: The DM values for each actuator will be stored as floating-point values in nanometers in the software.
- Initial DM values — used to achieve the initial contrast.
- DM drift — a random normally distributed value will be added to the state of each actuator between iterations. The values will be spatially and temporally uncorrelated, and the standard deviation of the drift will be kept constant across actuators and throughout the experiment (between 0.01 and 1 nm). The DM drift will not be passed to the wavefront sensing and control algorithms to simulate unpredictable wavefront instabilities.
- DM probes — random normally distributed values added to each actuator separately. These values will be passed to the estimation and control algorithms.
- Total DM displacement — the per-actuator sum of the initial DM values, accumulated DM drifts, and DM probes.

Deformable mirror voltages: The voltages passed to the DM mirrors which are converted from the total in-software DM displacement defined in the software.

Shot noise in HiCAT software: The values measured with the CMOS detector on HiCAT will be scaled to photon rate per iteration values. The scaling factor will be such that the average number of photons per pixel per iteration at the initial contrast will range from 0.09 (shot noise SNR=0.3) to 900 (SNR=30). The shot noise will then be simulated by sampling measurements from a Poisson distribution with the scaled photon rate as the parameter.

Shot noise on DST: To the extent possible, we will use the photon counting mode on the DST and adjust the photon flux through exposure times and the introduction of ND filters. Only if we cannot achieve some of the SNR levels between 0.3 and 30 will we resort to adding shot noise in the software in the same manner as with HiCAT.

Steady-state contrast: steady-state contrast will be computed as the average contrast after the wavefront control transients have subsided. In our previous experiment (see Fig. 2), the controller converged after about 50 iterations if it converged at all (since the DM dither was chosen too small). In this work, we will empirically determine the maximum number of iterations N it takes the convergent DHM experiments to converge, then take the average contrast of iterations N through 1.5 x N as the steady state contrast.

Contrast delta: the difference between the steady-state contrast and the initial contrast.

Incoherent background: Both HiCAT and DST introduce some light into the dark hole that cannot be modulated by the DM. Both HiCAT and DST also exhibit noise that arises at the detectors (e.g., dark current). The sum of these sources will be considered an "incoherent background."

Theoretical bound on contrast delta: theoretical bound on contrast delta is computed via an iterative procedure described in Pogorelyuk et al. 2021. The inputs to this procedure are the model-simulated dark hole properties as well as DM drift, shot noise values, and incoherent background.

6.2 Milestone Demonstration Procedure

Before running testbed experiments, optical models of HiCAT and the DST will be used to compute a theoretical bound on the closed-loop contrast delta for a range of DM drifts and shot noise SNR (see Sec. 4). Each experiment starts with a dark hole creation procedure that is standard for the given testbed (HiCAT or DST). Before each control iteration within the experiment, DM probes are introduced, and after each iteration, DM drift and shot noise (if necessary) are introduced. Wavefront estimation and the control loop are then closed using dark hole images and DM probes. If contrast converges, steady-state contrast and contrast delta are computed.

The testbeds and algorithms differ between milestones, as described in Table 1. For each set of DM drift and shot noise values, the experiments will be run several times in order to fine-tune the estimation and control algorithms to achieve best steady-state contrast. The best contrast delta across all algorithm tuning parameters will be recorded and compared to the theoretical bound.

6.3 Milestone Data Package

- A report that specifies the hardware employed during the experiments and its configuration, the algorithms used and their parameters, representative contrast time plots (for selected drift and noise parameters), comparison of contrast delta to theoretical predictions (for a range of drift and noise parameters), and how the milestone was met.
- At least three sets of DHM runs on HiCAT that include: sensor images. images with add noise, DM drift commands, DM probe commands, total DM commands, and DM electric field Jacobian.

7 Success Criteria

Experimental contrast delta on HiCAT with baseline algorithms at a starting contrast of 8×10^{-8} or better and for a range of conditions specified in Sec. 4.1. This initial study will quantify the gap between state-of-the-art DHM testbed performance and theoretical limits.

Experimental contrast delta on HiCAT within a factor of 5 of theoretical predictions with advanced algorithms for subset conditions as specified in Sec. 4.2. This provides an agreement between theory and experiments at 8×10^{-8} contrast level or better and provides an experience that will be useful for DST.

Experimental contrast delta on DST with baseline algorithms for a range of DM drift and shot noise parameters (TBD); This will be the first demonstration of closed-loop high-order wavefront control in the presence of time-varying wavefront errors at contrast better than 8×10^{-10}.

Experimental contrast delta on DST (in vacuum) within a factor of 5 of theoretical predictions with advanced algorithms for a range of parameters (TBD); This will achieve the success criteria of TRL 4 for contrast stabilization.

8 Schedule

Description	Completion Date
Precursor work: TRL 3 demonstration of DHM on HiCAT	2021
Theoretical predictions of close-loop contrast performance on HiCAT	June 2023
Basic DHM parameter scan on HiCAT parameter scan and comparison to theory	March 2024
Milestone 1	
Advanced DHM algorithms simulated on HiCAT model	March 2024
Theoretical predictions on close-loop contrast performance on DST	June 2024
Basic DHM simulated on DST model	September 2024
Advanced DHM parameter scan on HiCAT scan and comparison to theory	March 2025
Milestone 2	
Advanced DHM algorithms simulated on DST model	June 2025
Basic DHM implemented on DST	September 2025
Milestone 3	
Advanced DHM implemented on DST and parameter scan completed	December 2025
DST results analyzed and compared to theory and projections for HWO are made	March 2025
Milestone 4	

We note that the basic DHM algorithm will be simulated and ready to run on the DST by September 2024 — almost a year before it is scheduled to run on the testbed. To the extent that DST has availability before July 2025, we will start troubleshooting basic DHM on DST in monochromatic light and then in Roman-like setup or fully broadband light (see Sec. 5.3). If broadband basic-DHM experiments do not run on the DST by September 2025, they will be descoped in favor of advanced DHM algorithms.

References

Coyle, Laura E., et al. "Achieved technology maturation of key component-level technologies for ultra-stable optical systems." *Space Telescopes and Instrumentation 2022: Optical, Infrared, and Millimeter Wave*. Vol. 12180. SPIE, 2022.

Give'on, Amir, et al. "Electric field conjugation-a broadband wavefront correction algorithm for high-contrast imaging systems." *American Astronomical Society Meeting Abstracts*. Vol. 211. 2007.

Haffert, S. Y., et al. "Implicit electric field Conjugation: Data-driven focal plane control." *arXiv preprint arXiv:2303.13719* (2023).

Kasdin, N. Jeremy, et al. "The Nancy grace roman space telescope coronagraph instrument (CGI) technology demonstration." *Space Telescopes and Instrumentation 2020: Optical, Infrared, and Millimeter Wave*. Vol. 11443. SPIE, 2020.

Krist, John E. (2020). *Observing Scenario (OS) 9 time series simulations for the Hybrid Lyot Coronagraph Band 1.* https://wfirst.ipac.caltech.edu/sims/Coronagraph_public_images.html#CGI_OS9.

Laginja, Iva, et al. "Wavefront tolerances of space-based segmented telescopes at very high contrast: Experimental validation." *Astronomy & Astrophysics* 658 (2022): A84.

Meeker, Seth R., et al. "The Twin decadal survey testbeds in the high contrast imaging testbed facility at NASA's jet propulsion laboratory." *Techniques and Instrumentation for Detection of Exoplanets X*. Vol. 11823. SPIE, 2021.

Pogorelyuk, Leonid, and N. Jeremy Kasdin. "Dark hole maintenance and a posteriori intensity estimation in the presence of speckle drift in a high-contrast space coronagraph." *The Astrophysical Journal* 873.1 (2019): 95.

Pogorelyuk, Leonid, et al. "Information-theoretical limits of recursive estimation and closed-loop control in high-contrast imaging." *The Astrophysical Journal Supplement Series* 256.2 (2021): 39.

Pogorelyuk, Leonid, et al. "Dark hole maintenance with modal pairwise probing in numerical simulations of Roman coronagraph instrument." *Journal of Astronomical Telescopes, Instruments, and Systems* 8.1 (2022): 019002-019002.

Prada, Camilo Mejia, Eugene Serabyn, and Fang Shi. "High-contrast imaging stability using MEMS deformable mirror." *Techniques and Instrumentation for Detection of Exoplanets IX*. Vol. 11117. SPIE, 2019.

Pueyo, Laurent A., et al. "Fundamental limits of high contrast imaging with continuous WFS&C control in space." *Techniques and Instrumentation for Detection of Exoplanets X*. Vol. 11823. SPIE, 2021.

Redmond, Susan F., et al. "Dark zone maintenance results for segmented aperture wavefront error drift in a high contrast space coronagraph." *Techniques and Instrumentation for Detection of Exoplanets X*. Vol. 11823. SPIE, 2021.

Redmond, Susan F., et al. "Implementation of a dark zone maintenance algorithm for speckle drift correction in a high contrast space coronagraph." *Journal of Astronomical Telescopes, Instruments, and Systems* 8.3 (2022): 035001-035001.

Riggs, AJ Eldorado, et al. "Fast linearized coronagraph optimizer (FALCO) I: a software toolbox for rapid coronagraphic design and wavefront correction." *Space Telescopes and Instrumentation 2018: Optical, Infrared, and Millimeter Wave*. Vol. 10698. SPIE, 2018.

Ruane, Garreth, et al. "Broadband vector vortex coronagraph testing at NASA's high contrast imaging testbed facility." *Space Telescopes and Instrumentation 2022: Optical, Infrared, and Millimeter Wave*. Vol. 12180. SPIE, 2022.

Seo, Byoung-Joon, et al. "Testbed demonstration of high-contrast coronagraph imaging in search for Earth-like exoplanets." *Techniques and Instrumentation for Detection of Exoplanets IX*. Vol. 11117. SPIE, 2019.

Soummer, Rémi, et al. "High-contrast imager for complex aperture telescopes (HiCAT): 8. Dark zone demonstration with simultaneous closed loop low-order wavefront sensing and control." *Space Telescopes and Instrumentation 2022: Optical, Infrared, and Millimeter Wave*. Vol. 12180. SPIE, 2022.

Stark, Christopher C., et al. "ExoEarth yield landscape for future direct imaging space telescopes." *Journal of Astronomical Telescopes, Instruments, and Systems* 5.2 (2019): 024009-024009.

Sun, He, N. Jeremy Kasdin, and Robert Vanderbei. "Identification and adaptive control of a high-contrast focal plane wavefront correction system." *Journal of Astronomical Telescopes, Instruments, and Systems* 4.4 (2018): 049006-049006.